Physics Letters A 381 (2017) 597–603

Contents lists available at ScienceDirect

Physics Letters A

www.elsevier.com/locate/pla

Hindmarsh–Rose model: Close and far to the singular limit

Roberto Barrio [a,b,*], Santiago Ibáñez [c], Lucía Pérez [c]

[a] Departamento de Matemática Aplicada and IUMA, University of Zaragoza, E-50009 Zaragoza, Spain
[b] Computational Dynamics group, University of Zaragoza, E-50009 Zaragoza, Spain
[c] Departamento de Matemáticas, University of Oviedo, E-33007 Oviedo, Spain

ARTICLE INFO

Article history:
Received 12 August 2016
Received in revised form 9 December 2016
Accepted 10 December 2016
Available online 15 December 2016
Communicated by C.R. Doering

Keywords:
Hindmarsh–Rose model
Singular limit
Slow-fast dynamics
Spike-adding

ABSTRACT

Dynamics arising in the Hindmarsh–Rose model are considered from a novel perspective. We study qualitative changes that occur as the time scale of the slow variable increases taking the system far from the slow-fast scenario. We see how the structure of spike-adding still persists far from the singular case but the geometry of the bifurcations changes notably. Particular attention is paid to changes in the shape of the homoclinic bifurcation curves and the disappearance of Inclination-Flip codimension-two points. These transformations seem to be linked to the way in which the spike-adding takes place, the changing from fold/hom to fold/Hopf bursting behavior and also with the way in which the chaotic regions evolve as the time scale of the slow variable increases.

1. Introduction

It is out of discussion that to understand such a complex mechanism as the brain, and in general any living neural network, it is compulsory to know first the working of its basic building blocks: the neurons. Since the seminal contribution of Hodgkin and Huxley [1], neurons are commonly viewed as dynamical systems. Elements of bifurcation theory play an essential role in this context and help to understand neuronal activity.

The range of activity types that a neuron can exhibit is quite broad and includes quiescence (the state of not firing), tonic spiking, bursting and irregular (or chaotic) spiking. Each of these behaviors has its counterpart in the language of dynamical systems, either as stable periodic or chaotic orbits. Even the process of spike-adding can be linked to specific codimension-two homoclinic bifurcations (Orbit-Flip and Inclination-Flip points) and also to the so called canard explosions [2,3].

Hindmarsh–Rose (HR in the sequel) equations

$$\begin{cases} x' = y - ax^3 + bx^2 + I - z, \\ y' = c - dx^2 - y, \\ z' = \varepsilon(s(x - x_0) - z) \end{cases} \tag{1}$$

were introduced in [4] as a reduction of the Hodgkin–Huxley model. The HR model is simpler but it captures the main dynamical behaviors which are displayed by real neurons: quiescence, tonic spiking, bursting and irregular spiking (see [5–13]). The system possesses two time scales: x and y evolve as fast variables while z does it as a slow variable (so, it is a slow-fast dynamical system). The x variable should be treated as the voltage across the cell membrane, while the y and z variables would describe kinetics of some ionic currents. The *small* parameter ε controls the time scale of z and x_0 controls the rest potential of the system.

Different choices of the parameters have been considered in the literature (see [11] for an excellent review of the dynamics of the model). Following [2,11,12] we assume that

$$a = 1, \quad c = 1, \quad d = 5, \quad s = 4, \quad \text{and} \quad x_0 = -1.6. \tag{2}$$

With this choice, (1) becomes a family dependent only on parameters (b, I, ε). These parameters will be our primary bifurcation parameters.

In this paper we pay attention to the changes in the global picture as ε varies. From a realistic point of view it is clear that only small values of ε are of interest: typically $\varepsilon \ll 1$. We include a preliminary study about the singular limit of some relevant bifurcations. Nevertheless, in contrast with other approaches, we want to emphasize that the understanding of the bifurcation diagram for higher values of the slow time scale should be a crucial ingredient to get a whole picture of the dynamics and also it helps to understand what happens for $\varepsilon < 1$ (and not only $\varepsilon \ll 1$).

The article is arranged as follows: In Section 2 we compute the singular limit of the Hopf bifurcations as $\varepsilon \searrow 0$. Moreover, we show with numerical evidences that a singular limit also exists for the homoclinic bifurcation curves. We compare our results with

* Corresponding author at: Departamento de Matemática Aplicada and IUMA, University of Zaragoza, E-50009 Zaragoza, Spain.
E-mail addresses: rbarrio@unizar.es (R. Barrio), mesa@uniovi.es (S. Ibáñez), lpcuadrado@gmail.com (L. Pérez).

http://dx.doi.org/10.1016/j.physleta.2016.12.027
0375-9601/

those in [14–16] where similar singular limits were studied in a different model. In section 3 we investigate how the homoclinic bifurcation curves change as ε increases from small (slow-fast dynamics) to large values. We will see that, although the geometry of the bifurcation curves changes rapidly, many common features seem to persist. Section 4 is devoted to show how the global picture of spike-adding, bursting and chaotic behavior, bounded inside a loop formed by the Hopf bifurcation curves, evolves with ε. We will describe how this evolution seems to be linked to the changes along the homoclinic bifurcation curves. A summary is presented in Section 5. All continuations of bifurcation curves have been done with the free software AUTO [17,18].

2. Singular limits: Hopf bifurcation and homoclinic bifurcation

It easily follows (fixing all parameters but (b, I, ε)) that the equilibrium points of (1) are given by

$$y = 1 - 5x^2, \qquad z = 4(x + 1.6), \tag{3}$$

with x any real root of

$$P(x) = I - 5.4 - 4x + (b - 5)x^2 - x^3. \tag{4}$$

The Jacobian at a given equilibrium point is given by

$$\begin{pmatrix} -3x^2 + 2bx & 1 & -1 \\ -10x & -1 & 0 \\ 4\varepsilon & 0 & -\varepsilon \end{pmatrix}, \tag{5}$$

with characteristic polynomial

$$Q(\lambda) = \lambda^3 + q_2(x, b, \varepsilon)\lambda^2 + q_1(x, b, \varepsilon)\lambda + q_0(x, b, \varepsilon),$$

where

$$q_2(x, b, \varepsilon) = 3x^2 - 2bx + 1 + \varepsilon,$$
$$q_1(x, b, \varepsilon) = 3x^2 + (10 - 2b)x + \varepsilon(3x^2 - 2bx + 5),$$
$$q_0(x, b, \varepsilon) = \varepsilon\big(3x^2 + (10 - 2b)x + 4\big).$$

Necessary conditions for an Andronov–Hopf (AH) bifurcation are

$$P(x) = 0$$
$$C(x, b, \varepsilon) = q_2(x, b, \varepsilon)q_1(x, b, \varepsilon) - q_0(x, b, \varepsilon) = 0$$
$$q_1(x, b, \varepsilon) > 0.$$

The above conditions characterize a collection of surfaces on the space of parameters whose limit when $\varepsilon \searrow 0$ is given by

$$I - 5.4 - 4x + (b - 5)x^2 - x^3 = 0, \tag{6}$$
$$(3x^2 - 2bx + 1)\big(3x^2 + (10 - 2b)x\big) = 0, \tag{7}$$
$$3x^2 + (10 - 2b)x \geq 0. \tag{8}$$

Although the condition $q_1(x, b, \varepsilon) > 0$ is stated in terms of a strict inequality, we must consider the possibility of a non strict inequality at the limit when $\varepsilon \searrow 0$. The set S of points satisfying the above conditions consists of three curves as depicted (dashed blue) in Fig. 1. AH bifurcations curves for $\varepsilon = 0.005$ are also shown. Note that not the whole set S becomes the singular limit for AH bifurcations curves. When $x = 2(b - 5)/3$, (7) is satisfied and substituting in (6) we get the equation for the graph G of a polynomial $I(b)$ of degree 3. On the other hand, (8) is also satisfied because $3x^2 + (10 - 2b)x = 0$. It follows that G is the singular limit for a surface in the 3-parameter space satisfying $P(x) = 0$ and $C(x, b, \varepsilon) = 0$, but only a part of it satisfies $q_1(x, b, \varepsilon) > 0$. We note that the bifurcation diagram of the HR-model does not display a U-shaped Hopf bifurcation curve as that observed for other excitable systems (see [14–16,19]).

Fig. 1 also shows four homoclinic bifurcation curves (green and black) for different values of ε. The lowest value (black) is for

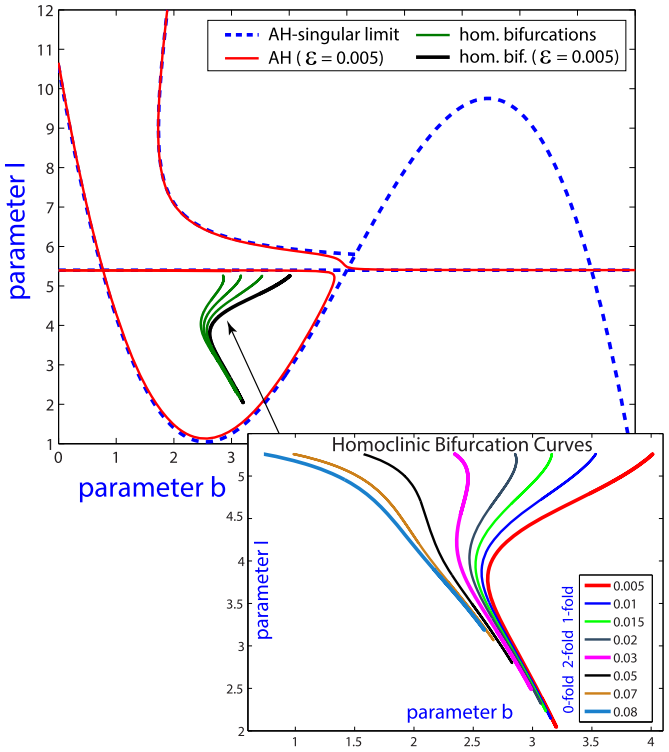

Fig. 1. Some features of the bifurcation diagram for the Hindmarsh–Rose model. Dashed blue curves show the set S of curves satisfying (6), (7) and (8), which contains the singular limit ($\varepsilon = 0$) of AH bifurcations in the full system. AH bifurcations (solid red) are shown for $\varepsilon = 0.005$. Note that not the whole set S is part of the singular limit. Homoclinic bifurcations (solid green and black) are shown for different values of ε (the lowest value (black) corresponds to $\varepsilon = 0.005$). In the magnification the first primary homoclinic bifurcations curves are shown for different values of ε. As the small parameter ε increases, the number of "visible" foldings (with respect to b) of the homoclinic curve changes. (For interpretation of the colors in this figure, the reader is referred to the web version of this article.)

$\varepsilon = 0.005$. In this case (for small values of ε), as for the systems considered in [14–16,19], homoclinic bifurcation curves are C-shaped. Numerical simulations show that there is a singular limit for the homoclinic bifurcations. Nevertheless, unlike the model studied in [15], a characterization of such singular limit involves extra difficulties and we pose this question as an open question for the next future. Anyway, it must be noticed that, as in [2,15], according to the numerical simulations, the homoclinic bifurcations curves do not terminate at a point approaching the set S. On the contrary, at both "ends" there is a sharp turning of the curve. However, this will make clear in the next section.

3. Homoclinic bifurcations

Of course, as already argued, an essential piece to get the whole picture of the dynamics emerging in the HR-model is to understand the role of the singular limit as the source of a puzzling bifurcation diagram. Nevertheless, to have a deeper knowledge of the model, it is also crucial to study a wider range of time scales of the slow variable z. In this approach, the latest goal should be to find organizing centers located not necessarily close to the singular limit and to understand how the bifurcations evolve as ε decreases. Hence, from a different perspective, this approach could be helpful to give some insight into the global picture that we already know to be very entangled for $\varepsilon \ll 1$.

Since this paper focuses mainly on the role played by the homoclinic bifurcation, we study how they evolve as ε varies (in this paper we just show the first primary homoclinic orbits, related with the first spike-adding process [2]). The numerical results dis-

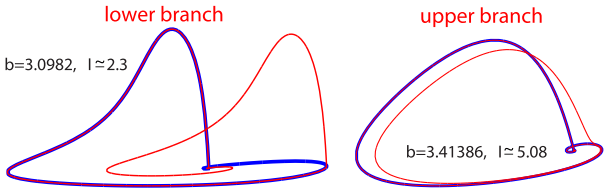

Fig. 2. Homoclinic orbits for parameter values in each of the two branches arising close to the lower and upper "endings or turning-points" of the homoclinic bifurcation curve for $\varepsilon = 0.01$. The selected value of b is the same in both cases of each branch, but the values of I corresponding to each homoclinic orbit (red and blue in each case) are slightly different as they correspond to different orbits of the double-cover homoclinic. (For interpretation of the colors in this figure, the reader is referred to the web version of this article.)

played in Fig. 1 show that the shape of the homoclinic bifurcations curves changes as ε increases. At this scale we clearly see three different shapes that we classify according to the number of "visible" folds in parameter b (the reason to say "visible" will be clear later). For ε small enough there is only one visible folding; these are the C-shaped curves already mentioned in Section 2 (the "standard" shape for slow-fast-systems [14–16,19]). For intermediate values there are two visible folding points in b, and as ε increases both visible foldings disappear. Moreover, an extra (and different) folding occurs at each "end" of the different branches of the homoclinic curves, giving a very sharp turn and so the curve doubles back on itself giving rise to a double-cover homoclinic curve (as shown in [2] for one value of ε). Fig. 2 shows two different homoclinic orbits obtained for parameter values at different branches at the lower and upper sharp folds (the value b is the same in both cases but the values of I are slightly different). The shape and relative position of the lower fold seems to be similar in all cases we have explored. On the contrary, the upper fold moves significatively in the biparametric plot as ε increases, as Fig. 1 shows.

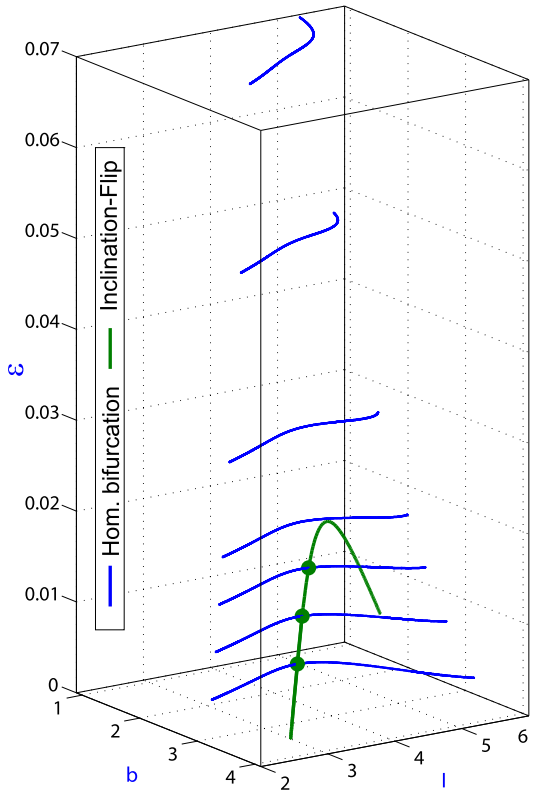

Fig. 3. A three-parametric plot (ε on the vertical axis) with the first primary homoclinic bifurcation curves (blue lines) at different values of ε and a three-parameter continuation of the curve (green line) of the codimension-two Inclination-Flip points. (For interpretation of the colors in this figure, the reader is referred to the web version of this article.)

4. Spike-adding and homoclinic bifurcations

From the observations of the previous section a clear question is: which consequences (if any) have the change of shape of the first primary homoclinic bifurcations curves?

First we remark that several recent works [2,5,6,11,12] were specifically focused on detailed studies of global bifurcations of tonic spiking and bursting orbits giving rise to chaotic dynamics in the HR model. In [2,6], the appearance of Orbit-Flip (OF) and Inclination-Flip (IF) codimension-two points in the primary homoclinic bifurcation curve was linked to the spike-adding process for square-wave (or fold/hom) bursting. Also, in [6] it was shown how these points give rise to the different macro-chaotic regions and a global scheme was proposed.

In order to observe in more detail the changes depending on the small parameter we show in Fig. 3 a three-parametric plot (ε on the vertical axis) with the first primary homoclinic bifurcation curves (blue lines) at different values of ε and a three-parameter continuation of the curve (green line) of the codimension-two Inclination-Flip points. The IF points play a relevant role for small values of ε, as shown in [2,6], because they are organizing centers of the pencils of period-doubling and fold bifurcations emanating from the OF points. All these points provide a complete picture of the spike-adding process, but when ε grows the IF points disappear, and so now the global structure has changed. It is interesting to remark that the disappearance of the IF points seems to take place in a codimension-three "fold" of IF points close to the parameter values $b = 2.525$, $I = 4.348$ and $\varepsilon = 0.0197$. The curve of codimension-two IF points also disappears when ε decreases in one side of the curve, but this fact may be related with numerical precision problems (in Fig. 4 we present all the IF points detected by AUTO for the corresponding ε values). All these facts are part of the current research of the authors.

In order to observe the changes originated from the disappearance of the IF points we use another very interesting approach, the spike-counting (SC) method, that works well for a neuron model when a bursting solution follows closely the slow motion manifolds of the fast subsystem and makes pronounced rapid jumps between them, thus defining the number of spikes per bursts in the voltage traces. Indeed, the spike number within a burst is that of the complete revolutions of the bursting orbit around the spiking manifold M_{lc}. In the spike-counting technique [5,12], a fixed number of spikes per burst is an indication of regular bursting, while unpredictably varying numbers are associated with chaotic bursting. Fig. 4 represents bi-parameter sweeps of the HR model in the (b, I)-plane for $\varepsilon = 0.01$, 0.03 and 0.05, that are done with the spike-counting approach. The parameter plane is clearly demarcated into regions corresponding to quiescence (convergence to an equilibrium point), periodic tonic spiking, chaotic and regular bursting. The obtained maps are color-coded, so, the spike numbers are associated with specific colors. The resulting diagram can be easily read and interpreted: the region shown in a dark blue color is for stable spiking activity which can be treated as bursting with a single spike. The diagram reveals a global organization of spike-adding bifurcations occurring on borderlines between the corresponding stripes in the blue hue, which all correspond to square-wave bursting on the model. Stripes of gradually changing colors correspond to bursting with incrementally varying numbers of spikes due to a spike-adding cascade. Bursting becomes chaotic near the transitions to tonic spiking in a chain of "onion bulb scales"- shaped regions [6]. Decreasing the value of ε, which determines the dynamics of the slow z-variable, does not change

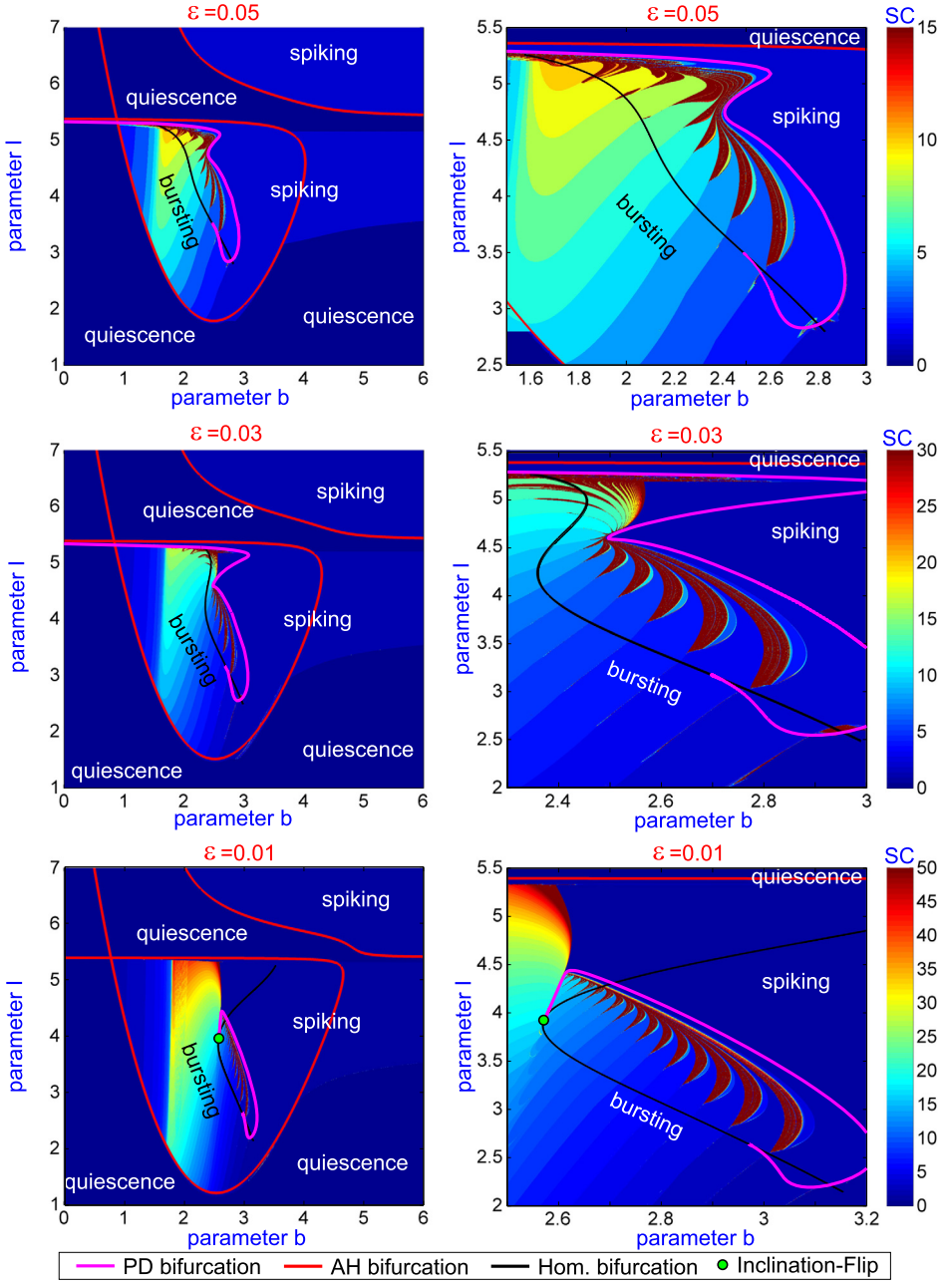

Fig. 4. Bi-parametric plot (plane (b, I)) of the HR-model at three values of ε, where the different colors indicate the number of spikes per period (spike-counting technique) and, superimposed, the bifurcation curves that demarcate the borderlines of the regions of colors ranging from blue to red and corresponding to spike numbers (vertical bar). Curves shown in pink, red and black correspond to period-doubling, Andronov–Hopf (AH) and primary homoclinic (Hom) bifurcations. The green dot corresponds to an Inclination-Flip codimension-two bifurcation point. Right column corresponds to a magnification of the bursting region. (For interpretation of the colors in this figure, the reader is referred to the web version of this article.)

qualitatively the structure of the parameter plane but compresses it. Therefore, for simplicity we do not consider values of $\varepsilon < 0.01$.

Detailed bifurcation analysis were presented in [6,12]. In this paper, as before, we just focus our attention into the AH and homoclinic bifurcations when different values of the small parameter ε are used. The AH-bifurcation curves do not change their shape, but, as shown in the previous section, the shape of the homoclinic bifurcation curve changes, passing from 1-fold (C-shape) in the b parameter to 2 (Z-shape) and later to 0. These changes originate also changes in the spike-adding process and in the chaotic regions. In all three cases, the spike-adding process follows the scheme shown in [2,6], but in the C-shape there is no spike-adding process in the upper branch, while in the other cases the spike-adding process continues and in the case of no "visible" folds the spike-adding is continued by a spike-deleting process. Also, the chaotic "onion bulbs" are present in the lower branch for the C-shape, whereas in the other two cases they are present along all the homoclinic bifurcation curve. Moreover, the change in the number of "visible" folds is located in the range of values of the parameter ε where the disappearance of the IF points (green dots) occurs. To study its relation with the change of the global picture we present also the first period-doubling curve (pink curve) that delimits the spiking region and we observe how, as the IF is no more present, the curve goes far away for high values of ε, whereas for small values the IF point attracts all these bifurcation curves.

The influence of the fact that the bifurcation curves end at the IF, or not, gives rise to another important feature. In Fig. 5

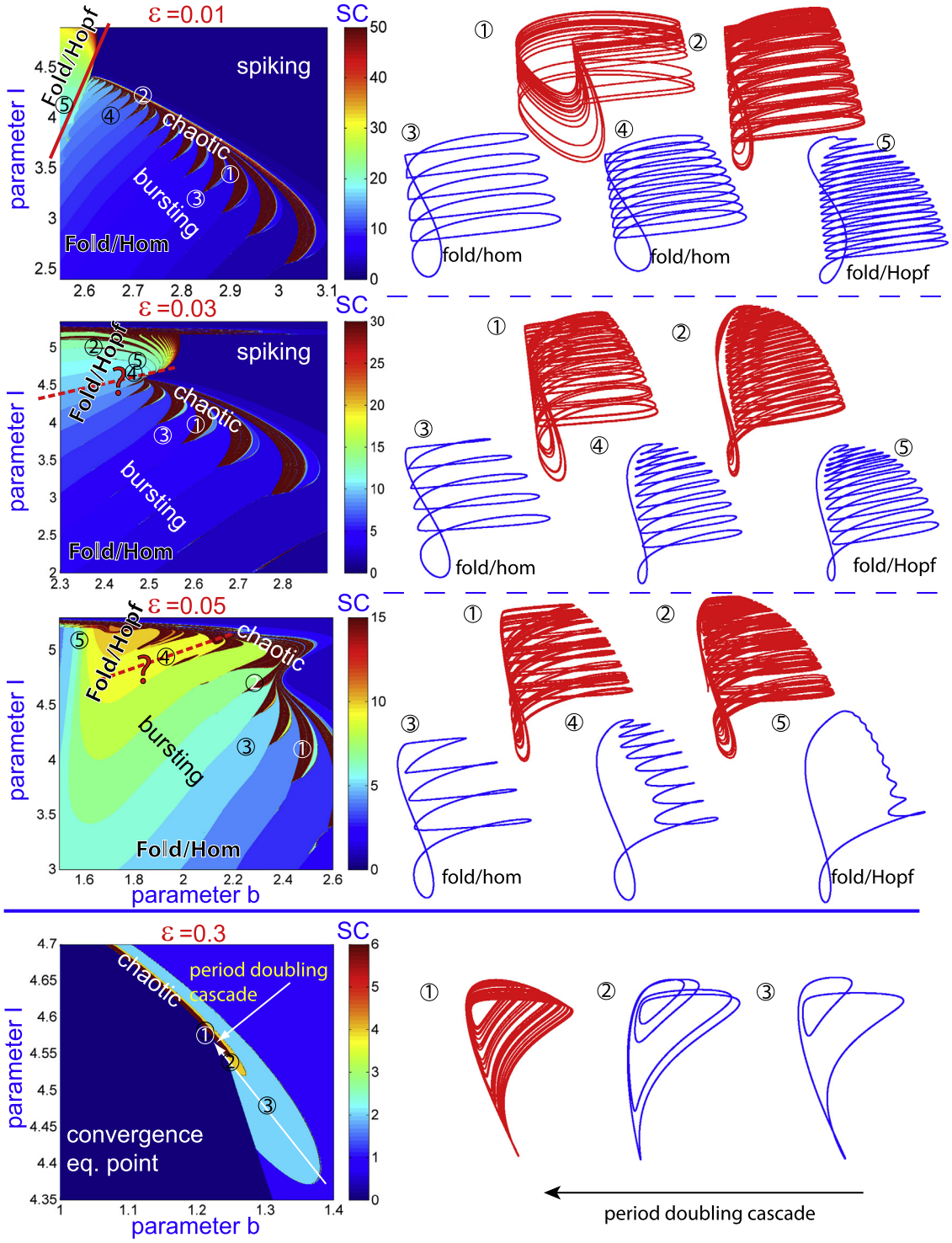

Fig. 5. Evolution of the orbits (stable periodic orbits (blue) and chaotic ones (red)) for different values of the parameter ε. On the left SC bi-parametric plots (plane (b, I)) showing the position of the different orbits and the change with ε in the spike-adding process and chaotic regions (in dark red). Regions with Fold/Hom and Fold/Hopf bursting behavior are shown (in case $\varepsilon = 0.01$ the regions are quite delineated, but in the other cases the change is more gradual without a clear boundary). (For interpretation of the colors in this figure, the reader is referred to the web version of this article.)

we present on the left the SC sweeping technique for four values of ε, in this case considering also a value clearly far from small ($\varepsilon = 0.3$). The case $\varepsilon = 0.01$ is clearly slow-fast, with the chaotic and periodic orbits with spikes around the fast spiking manifold M_{lc}. Moreover, if we observe the SC diagram there are two clearly defined areas in the bursting region (shown by the continuous straight red line that it is delined by the IF point and the bifurcation curves ending to it) of fold/hom (or square-wave) and fold/Hopf (or plateau-like) bursting behavior. The difference of the orbits is evident from the right figures. On the contrary, increasing the value of ε, as the IF point is no more present there is not a clear boundary. For $\varepsilon = 0.03$ and 0.05 we observe that now there is also fold/hom and fold/Hopf bursting behavior, but now we cannot give a precise limit of each behavior (so we have plotted a discontinuous red line with an interrogant on the area where the change seems to occur). This fact has clear biological interest as now there is a small change when varying the parameter as the geometry of the orbits is quite similar (when ε is small in the area of changing from fold/hom to fold/Hopf the difference is quite big). We also remark that, when ε grows, the dynamics of the system maintains some of the slow-fast features (spike-adding, chaotic stripes, ...) but now the spiking process is more and more similar to the funnel structures created around focus equilibria in Rössler-like systems (see [20]).

For large values of ε ($\varepsilon = 0.3$) we observe that the structure is not the same, and now the spike-adding process is not observed, being present a classical period-doubling phenomena giving rise to a small chaotic area, that is, now the system is not a slow-fast system, it is just another 3D dynamical system with oscillatory behavior around focus equilibria. The other three values of ε maintains some slow-fast dynamics.

A deep analysis of the changes from the limit case ($\varepsilon \searrow 0$) to the case $\varepsilon = \mathcal{O}(1)$ is part of our current research [21].

5. Conclusions

In this article, we present new approaches to study the dynamics arising in the HR model. Andronov–Hopf and homoclinic bifurcations play an essential role in the understanding of the whole picture. We have computed the singular limit of the Andronov–Hopf bifurcations in the family and checked that for each $\varepsilon > 0$ small, one of the Hopf bifurcation curves forms a loop which bounds all the rich variety of behaviors displayed by the system. This differs from other models considered in the literature where the Andronov–Hopf bifurcation curve (for fixed ε) adopts an U-shape as it tends to the singular limit (see [15]). On the other hand, although it is well known that homoclinic bifurcations of codimension-one or higher are key pieces in the organization of the bifurcations diagrams, this paper shows that this role extends from the singular limit up to, at least moderately, large values of ε. The variations in the shape of a principal homoclinic bifurcation curve were explored starting close to its singular limit and increasing the values of ε to get images of the behavior far from the slow-fast scenario. It becomes evident that close to the singular limit it adopts a C-shape with a unique principal "visible" folding point. As ε increases, the Inclination-Flip codimension-two points disappear, generating a smooth change from fold/hom and fold/Hopf bursting behavior. Moreover, although spike-adding and chaotic regions are present, the way in which new regions with differenced dynamics emerge is clearly different. The different shapes of the homoclinic bifurcation curves seem to be related to these changes in the dynamics.

As already mentioned, our current research is addressed to get a deeper insight in the manner in which the whole bifurcation diagram evolves as ε moves in a long interval. This should also gives us some enlightenment in the understanding of the slow-fast mechanisms that explain the fascinating variety of neuronal activities. Regarding this point, it will be necessary to complete the study of singular limits, particularly, for the case of homoclinic bifurcation curves. Moreover, new codimension-two organizing centers need to be detected. For instance, it is still far from being clear which are the bifurcations existing at the terminal points of homoclinic bifurcation curves.

Acknowledgements

R.B. has been supported during this research by the Spanish Research projects MTM2012-31883 and MTM2015-64095-P (MINECO/FEDER) and the European Social Fund and Diputación General de Aragón (Grant E48). S.I. has been supported by the Spanish Research project MTM2014-56953-P. The authors thank the reviewers for their constructive remarks.

References

[1] A.L. Hodgkin, A.F. Huxley, A quantitative description of membrane current and its application to conduction and excitation in nerve, J. Physiol. 117 (1952) 500–544.
[2] D. Linaro, A. Champneys, M. Desroches, M. Storace, Codimension-two homoclinic bifurcations underlying spike adding in the Hindmarsh–Rose burster, SIAM J. Appl. Dyn. Syst. 11 (3) (2012) 939–962.
[3] M. Desroches, T.J. Kaper, M. Krupa, Mixed-mode bursting oscillations: dynamics created by a slow passage through spike-adding canard explosion in a square-wave burster, Chaos 23 (4) (2013) 046106, http://dx.doi.org/10.1063/1.4827026.
[4] J.L. Hindmarsh, R.M. Rose, A model of neuronal bursting using three coupled first order differential equations, Proc. R. Soc. Lond. B, Biol. Sci. 221 (1222) (1984) 87–102, http://dx.doi.org/10.1098/rspb.1984.0024.
[5] R. Barrio, A. Shilnikov, Parameter-sweeping techniques for temporal dynamics of neuronal systems: case study of Hindmarsh–Rose model, J. Math. Neurosci. 1 (2011) 6.
[6] R. Barrio, M. Angeles-Martínez, S. Serrano, A. Shilnikov, Macro- and microchaotic structures in the Hindmarsh–Rose model of bursting neurons, Chaos 24 (2) (2014), http://dx.doi.org/10.1063/1.4882171.
[7] J.M. González-Miranda, Observation of a continuous interior crisis in the Hindmarsh–Rose neuron model, Chaos 13 (3) (2003) 845–852, http://dx.doi.org/10.1063/1.1594851.
[8] J.M. González-Miranda, Complex bifurcation structures in the Hindmarsh–Rose neuron model, Int. J. Bifurc. Chaos 17 (09) (2007) 3071–3083, http://dx.doi.org/10.1142/S0218127407018877.
[9] G. Innocenti, A. Morelli, R. Genesio, A. Torcini, Dynamical phases of the Hindmarsh–Rose neuronal model: studies of the transition from bursting to spiking chaos, Chaos 17 (4) (2007) 043128, http://dx.doi.org/10.1063/1.2818153.
[10] G. Innocenti, R. Genesio, On the dynamics of chaotic spiking-bursting transition in the Hindmarsh–Rose neuron, Chaos 19 (2) (2009) 023124, http://dx.doi.org/10.1063/1.3156650.
[11] A. Shilnikov, M. Kolomiets, Methods of the qualitative theory for the Hindmarsh–Rose model: a case study. A tutorial, Int. J. Bifurc. Chaos 18 (8) (2008) 2141–2168.
[12] M. Storace Linaro, E. de Lange, The Hindmarsh–Rose neuron model: bifurcation analysis and piecewise-linear approximations, Chaos 18 (2008) 033128.
[13] D. Terman, Chaotic spikes arising from a model of bursting in excitable membranes, SIAM J. Appl. Math. 51 (5) (1991) 1418–1450, http://dx.doi.org/10.1137/0151071.
[14] A.R. Champneys, V. Kirk, E. Knobloch, B.E. Oldeman, J. Sneyd, When Shil'nikov meets Hopf in excitable systems, SIAM J. Appl. Dyn. Syst. 6 (4) (2007) 663–693, http://dx.doi.org/10.1137/070682654.
[15] J. Guckenheimer, C. Kuehn, Homoclinic orbits of the FitzHugh–Nagumo equation: the singular-limit, Discrete Contin. Dyn. Syst. 2 (4) (2009) 851–872, http://dx.doi.org/10.3934/dcdss.2009.2.851.
[16] J. Guckenheimer, C. Kuehn, Homoclinic orbits of the FitzHugh–Nagumo equation: bifurcations in the full system, SIAM J. Appl. Dyn. Syst. 9 (1) (2010) 138–153, http://dx.doi.org/10.1137/090758404.
[17] E.J. Doedel, R. Paffenroth, A.R. Champneys, T.F. Fairgrieve, Y.A. Kuznetsov, B.E. Oldeman, B. Sandstede, X.J. Wang, AUTO2000, http://cmvl.cs.concordia.ca/auto.
[18] E. Doedel, AUTO: a program for the automatic bifurcation analysis of autonomous systems, in: Proceedings of the Tenth Manitoba Conference on Numerical Mathematics and Computing, Vol. I, Winnipeg, Man., 1980, vol. 30, 1981, pp. 265–284.
[19] J. Guckenheimer, H.M. Osinga, The singular limit of a Hopf bifurcation, Discrete Contin. Dyn. Syst. 32 (8) (2012) 2805–2823, http://dx.doi.org/10.3934/dcds.2012.32.2805.

[20] R. Barrio, F. Blesa, S. Serrano, Qualitative analysis of the Rössler equations: bifurcations of limit cycles and chaotic attractors, Phys. D 238 (2009) 1087–1100.

[21] R. Barrio, S. Ibáñez, L. Pérez, Different spike-adding processes in neuron models, preprint.